Bull. Inst. Chem. Res., Kyoto Univ., Vol. 52, No. 2, 1974

The Mechanical and Rheo-Optical Properties of Nylon 11 and 12

Shigeharu ONOGI, Tadahiro ASADA, Yoshiharu FUKUI*,
and Isao TACHINAKA**

Received March 4, 1974

In order to understand the deformation mechanisms in nylon 11 and 12 in the primary dispersion region, rheo-optical and mechanical properties of these materials were measured over wide ranges of time-scale and temperature.

In marked contrast to the strain-optical coefficients for polyethylene and polypropylene, which were studied previously, those for nylon 11 and 12 decrease with increasing time during relaxation measurements. Moreover, the strain-optical coefficient at 1 sec decreases continuously with temperature and does not show the peak which is typical of polyethylene.

The amorphous contribution to the total birefringence was also determined by making visible dichroism measurements on films dyed with congo red. The amorphous birefringence increases with increasing time, from which it follows that the crystalline birefringence must be decreasing enormously with time in order to override the effect of the amorphous phase. As expected, the infrared dichroism for the crystalline bands at around 940 cm^{-1} decreases with increasing time, though the effect is not large enough to override the increasing behavior of the amorphous phase.

The activation energy for the relaxation process in the primary dispersion region was found to be about 60 kcal/mole, as determined from rheo-optical and viscoelastic shift factors used in the time-temperature superposition procedure.

The above results indicate that the nylons show a quite different crystalline structure, and hence different rheo-optical properties, than do the polyolefins.

INTRODUCTION

The studies on the rheo-optical properties of polyethylene and polypropylene which have been carried out in Dr. Stein's and our laboratories[1] over the past decade have shown that the rheo-optical and viscoelastic properties of undrawn polyolefins can be well-explained by considering three deformation mechanisms: the deformation of the spherulites as a whole, the orientation of crystals in the spherulites, and the orientation of amorphous molecular chains. These mechanisms were proposed by us in an earlier paper published in 1964[2]. Among the three, crystalline orientation produces certain birefringence effects (for example, in the case of polyethylene, an increase in birefringence with time during stress relaxation or a decrease in dynamic birefringence with frequency) which seem to be peculiar to the polyolefins. In contrast to the behavior of polyethylene, Yamada and Stein reported in the case of nylon 6 that the dynamic birefringence or strain-optical coefficient increases with frequency[3]. Yamada, Hayashi, and Onogi[4] also showed that the dynamic strain-optical coefficient for nylon 6 and polyvinyl alcohol increases with

* 小野木重治, 浅田忠裕, 福井芳治: Department of Polymer Chemistry, Faculty of Engineering, Kyoto University, Kyoto.

** 立中 勲: On Ieave from Toyo Kohan Co., Ltd., Tokyo.

frequency. Therefore, it appears that there may be a significant difference in the deformation (or orientation) mechanisms and also in the crystalline structure of polyolefins as compared with other crystalline polymers, especially those having a high cohesive energy density.

In the present work, nylon 11 and 12 were chosen as representative crystalline polymers for a comparison study, and their rheo-optical and mechanical properties were measured over wide ranges of time-scale and temperature in order to understand the deformation mechanisms in the primary dispersion region.

EXPERIMENTAL

Materials

Quenched and annealed films of nylon 11 and 12 were used in this study. The quenched films were prepared by extruding commercial nylons from a slot-die and cooling the extrudate very quickly on a chilled roller. The thickness of the films was about 50 μ for nylon 11 and about 55 μ for nylon 12.

To prepare the annealed films, the quenched films were put between two aluminum plates coated with silicone and then heated in a laboratory hot press for 30 min at various temperatures. The temperatures ranged from 100° to 185°C in the case of nylon 11 and from 100° to 175°C in the case of nylon 12. After heating the samples were cooled to room temperature.

Some of the films were dyed by soaking them in a 0.05% ethanol solution of congo red for one day followed by drying in a desiccator. Dichroism measurements were then carried out on the film specimens.

Measurements

The density of the films was measured by the floatation method in a toluene-carbon tetrachloride mixture at 30°C.

The stress relaxation and the birefringence relaxation measurements were made on the same instrument that was used previously[1]. It consists of an Instron-type tensile tester (Tensilon UTM-IV) combined with an optical system for measuring the birefringence continuously by an intensity method. For measuring dichroism, the analyzer was removed from the optical system and the polarizer was rotated such that its optical axis become parallel or perpendicular to the stretching direction of the film specimen.

The instrument for measuring infrared dichroism and absorption has been described previously[5,6]. The dynamic mechanical properties and the X-ray diffraction properties were also measured on instruments that have been described in earlier references[7,15].

RESULTS AND DISCUSSION

Characterization of Crystalline Structure

As is well-known, there are two different crystal modifications for nylon 11: the α (triclinic) modification and the γ (pseudohexagonal) modification[8~14]. It is also known that the γ modification changes into the α modification when the material is heated.

Figure 1 gives the X-ray diffraction intensity results for the quenched film of nylon

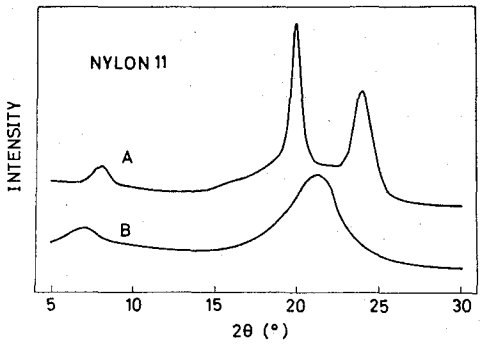

Fig. 1. X-ray diffraction intensity curves for the solution-cast film (A) and the quenched film (B) of nylon 11.

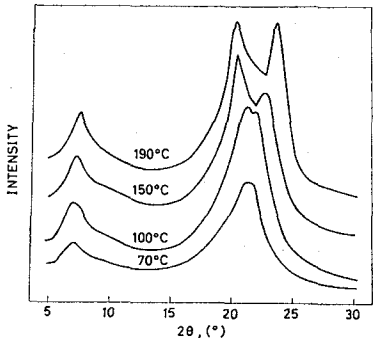

Fig. 2. X-ray diffraction intensity curves for nylon 11 films annealed at 70°, 100°, 150°, and 190°C.

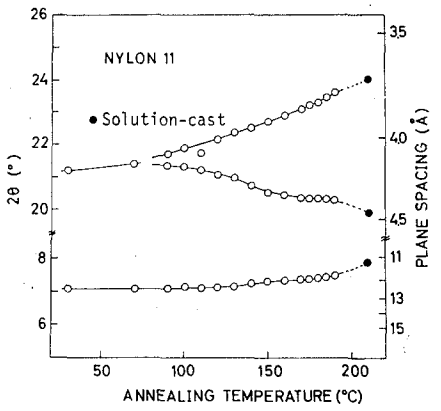

Fig. 3. The Bragg angles at which the peaks appear plotted against the annealing temperature.

11 (bottom curve). The curve shows two strong peaks at $2\theta=21.2°$ and at 7.1°, indicating that the film contains γ crystals. In the same figure, the X-ray diffraction results for a nylon 11 film cast from *m*-cresol solution are also shown (top curve). This curve has three distinct peaks, at $2\theta=24.0°$, at 19.9°, and at 7.9°, indicating that the solution-cast film contains α crystals.

Figure 2 gives X-ray diffraction curves for nylon 11 films which were annealed in a hot press for 30 min at 70°, 100°, 150°, and 190°C. By annealing at temperatures higher than 100°C, the peak at $2\theta=21.2°$ separates into two different peaks, indicating that a crystal transformation from the γ modification to the α modification occurred during the annealing process. The Bragg angles at which the peaks appear are plotted against the annealing temperature in Fig. 3. As is evident from this figure, the peak at $2\theta=21.2°$ separates into two peaks at temperatures higher than 90°C; the higher the temperature, the more the two peaks separate from each other. The limiting values for the Bragg angles of the two peaks are 24.0° and 19.9° (shown by the closed circles in the figure) corresponding to the α modification, similar in behavior to the solution-cast film noted previously. Another peak at $2\theta=7.1°$ shifts slightly to the wide-angle side as the temperature increased, until it reaches a limiting value of $2\theta=8°$ corresponding to the α modification. Thus, the γ modification in nylon 11 changes to the α modification when films are heated above 90°C.

In Fig. 4 are given the infrared absorption spectra for the quenched film (γ crystals) and the solution-cast film (α crystals). The most notable difference between the spectra for these two kinds of films can be seen around 700 cm^{-1}. Only the α crystals show an absorption band at 687 cm^{-1}.

For nylon 12, there are also α and γ modifications[11]. As can be seen in Fig. 5, the X-ray diffraction intensity curve (A) for the quenched film of nylon 12 is very similar to that for γ crystals in nylon 11 and has two peaks, at $2\theta=21.5°$ and at 6.0°. A film cast from *m*-cresol solution gives a curve (Fig. 5-B) different from that for the quenched film; the curve has three peaks, at $2\theta=24.1°$, at 20.2°, and at 6.1°. This type of crystals will be referred as to α crystals. The diffraction intensity curve has another faint peak at $2\theta=21.4°$, indicating that the solution-cast film contains a small amount of γ crystals. In Fig. 5, the x-ray diffraction intensity curve for the film annealed at 180°C is also compared with that for the quenched film. As is evident from this figure, the peaks at $2\theta=21.5°$

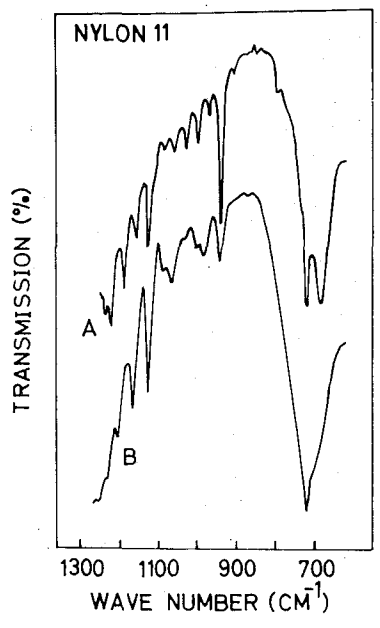

Fig. 4. The infrared absorption spectra for the solution-cast film (A) and the quenched film (B) of nylon 11.

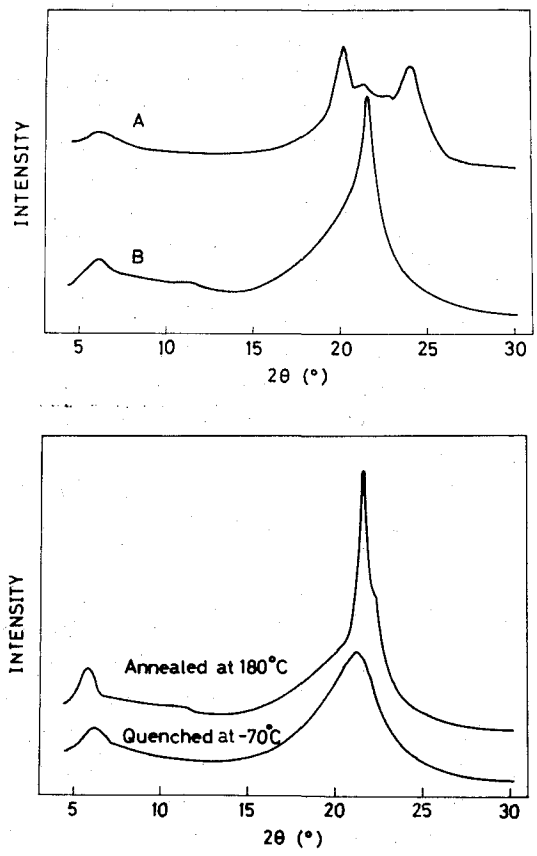

Fig. 5. X-ray diffraction intensity curves
[top] for the solution-cast film (A) and the quenched film (B) of nylon 12,
[bottom] for film quenched at −70°C and film annealed at 180°C.

and 6.0° for the quenched film are shifted, respectively, to $2\theta=21.7°$ and 5.8° after annealing. However, no change large enough to indicate the occurrence of a crystal transformation can be observed. From this result, it follows that γ crystals in nylon 12, in contrast to nylon 11, are very stable even when the film is annealed at high temperatures.

The densities measured at 30°C for the quenched and annealed films of nylon 11 and 12 are plotted against the annealing temperature in Fig. 6. The lowest densities in this figure are the same as those for the quenched films. The density, and hence the degree of crystallinity, increases rapidly with increasing annealing temperature. The degree of crystallinity corresponding to the lowest density is about 23% for nylon 11, and about 33% for nylon 12.

The Variation of Birefringence with Strain

First, the quenched films were elongated under a constant speed of 10%/min at various temperatures ranging from 30° to 160°C, and the birefringence and the stress were measured simultaneously as a function of strain. The quenched films of nylon 11 and 12 used in this study showed a slight initial orientation in the machine direction, and thus the birefringence in the unstrained state was not zero. This initial birefringence

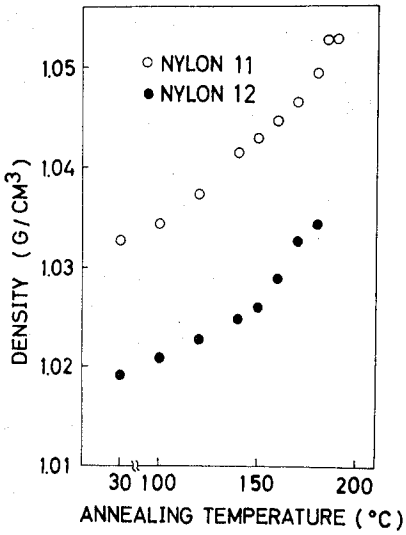

Fig. 6. The variation of density with annealing temperature.

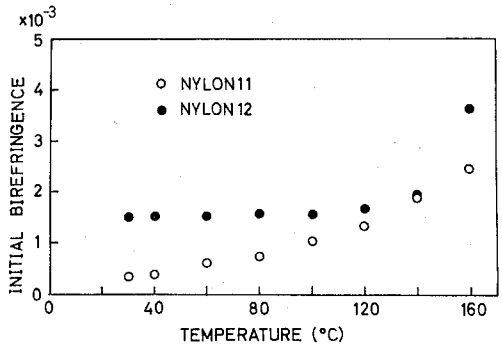

Fig. 7. The variation of initial birefringence with temperature for the quenched films of nylon 11 and 12.

varies with temperature, as is shown in Fig. 7. For simplicity, therefore, the initial birefringence was subtracted from all of the experimental values of birefringence reported below.

The stress-strain curves and birefringence-strain curves for the quenched nylon 11 film are given in Fig. 8. As is evident from this figure, the birefringence increases with strain, but the higher the temperature, the lower the birefringence becomes. This behavior is just opposite to that of polyethylene reported in a previous paper[15]. The stress also decreases with raising temperature. At 30° and 40°C, the film specimen showed necking during the measurements, but above 60°C it was elongated uniformly, showing no necking.

Similar results for nylon 11 films annealed for two hours at 140°C are given in Fig. 9. The birefringence decreases with increasing temperature, but the temperature dependence is not as large as in the case of the quenched film mentioned above. The stress-strain curves are shaped somewhat differently than those for the quenched film. Also, the yield stress and the strain at yield are considerably higher. In the case of nylon 11 such differences

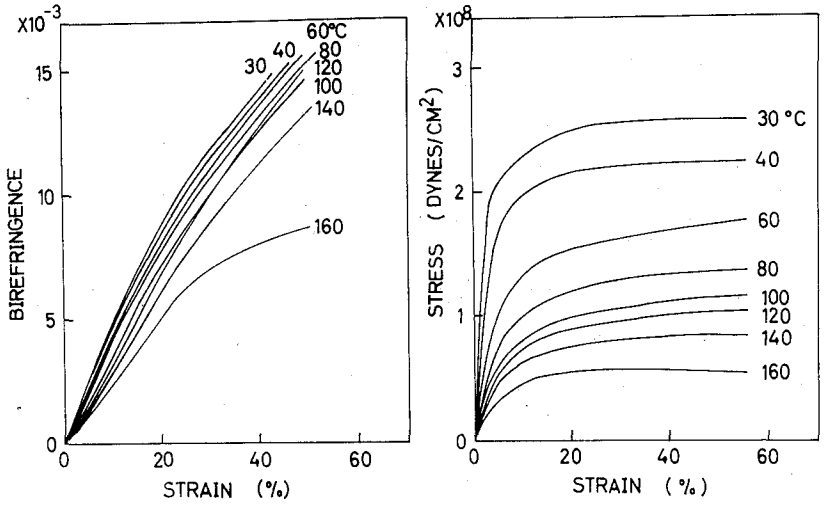

Fig. 8. Birefringence-strain and stress-strain curves for the quenched nylon 11 film.

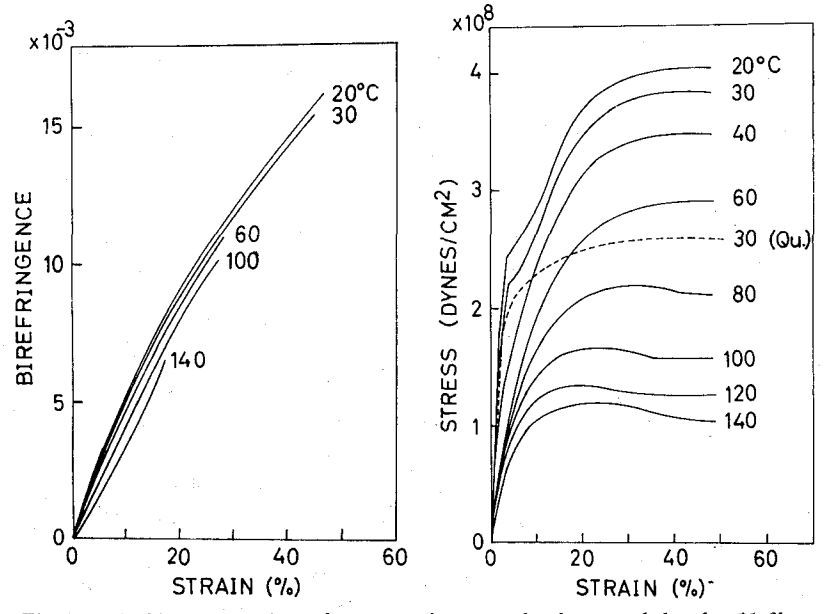

Fig. 9. Birefringence-strain and stress-strain curves for the annealed nylon 11 film.

are ascribed mainly to the difference in degree of crystallinity and partly to the crystal transformation which occurs during the annealing.

In Fig. 10 is shown the strain dependent variation of birefringence and of stress for the quenched film of nylon 12 at various temperatures. The birefringence decreases with rising temperature, similar to the case of nylon 11, but the temperature dependence for nylon 12 is larger than that for nylon 11. The corresponding stress-strain curves are also similar to, though not completely same as, those for nylon 11, with the biggest differences being seen in the temperature dependence.

The birefringence-strain and stress-strain curves for nylon 12 films annealed at

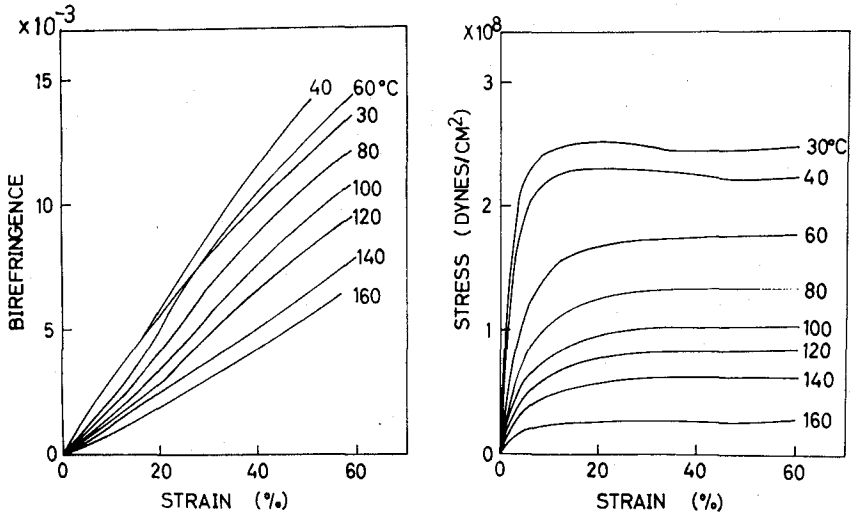

Fig. 10. Birefringence-strain and stress-strain curves for the quenched nylon 12 film.

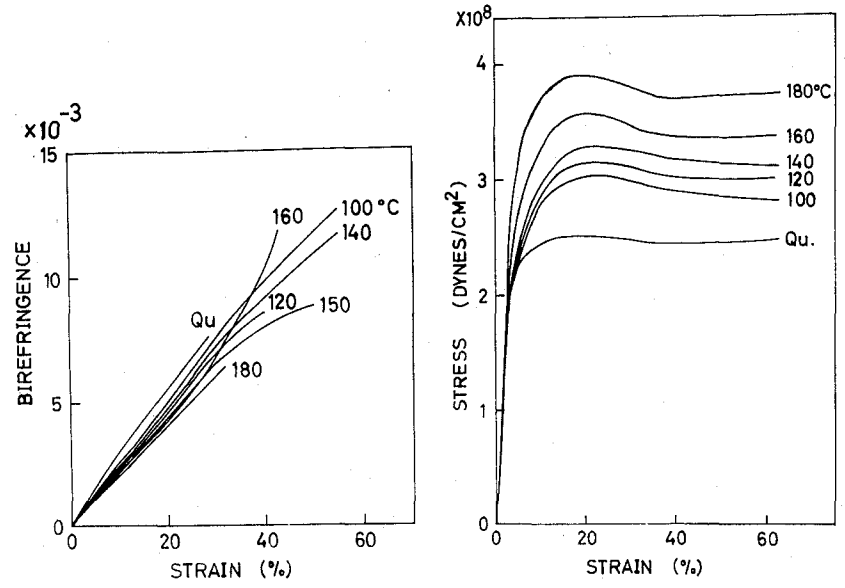

Fig. 11. A comparison of the birefringence-strain and stress-strain curves for nylon 12 films annealed at different temperatures with those for the quenched film (Qu).

different temperatures are compared with those for the quenched film in Fig. 11. As is evident from this figure, at a given strain the birefringence decreases and the corresponding stress increases as the annealing temperature is increased. As mentioned above, the density increases with increasing annealing temperature. Thus, the birefringence decreases with increasing degree of crystallinity. Such a relationship between the birefringence and the degree of crystallinity for the nylons is just the reverse of that for the polyethylenes, which suggests that the contribution of the crystalline phase to the total birefringence is not the same in the two cases.

The Temperature and Frequency Dependences of Dynamic Viscoelasticity

In connection with the rheo-optical behavior of nylon 11 and 12, the dynamic viscoelastic properties, and particularly the temperature dependences of these properties, will be described briefly.

The storage (E') and loss (E'') Young's moduli of the quenched films of nylon 11 and 12 were measured at 110 Hz at temperatures between −100° and 180°C and are plotted against temperature in Figs. 12 and 13. The so-called primary or α-dispersion can be seen at about 70°C for nylon 11 and at about 60°C for nylon 12, and the β-dispersion can be seen at about −50°C for both materials. Another dispersion observed near 160°C for nylon 11, appears to be α_c-dispersion.

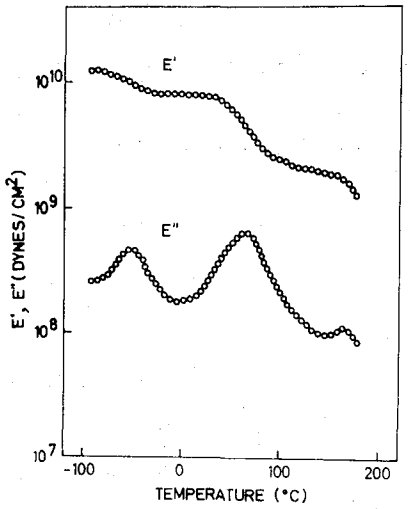

Fig. 12. Temperature dependence of the storage Young's modulus E' and loss modulus E'' at 110 Hz for the quenched film of nylon 11.

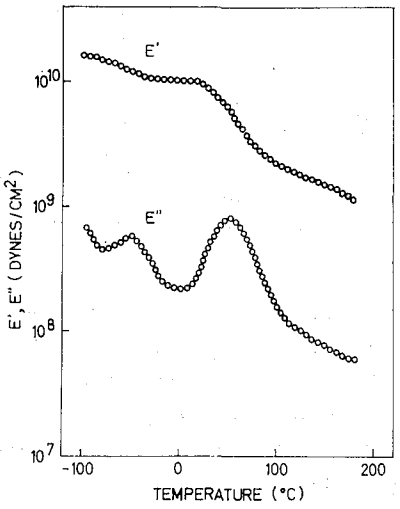

Fig. 13. Temperature dependence of the storage Young's modulus E' and loss modulus E'' at 110 Hz for the quenched film of nylon 12.

On the other hand, the properties of the annealed films are rather different, as may be seen in Fig. 14 which presents E' and E'' data for the films annealed at 185°C. Comparing this figure with Figs. 12 and 13, it is clear that E' is increases considerably by annealing. The temperature at which the α-dispersion peak of E'' is observed is also raised by several degrees by annealing. The temperature dependence of the loss tangent tanδ for the quenched and annealed films is shown in Fig. 15. The quenched films have higher α-dispersion peaks, but lower α_c-peaks, as compared with the annealed films.

In Figs. 16 and 17, E'' and tanδ measured at 110 Hz, 11 Hz, and 3.5 Hz for the quenched film of nylon 11 are plotted against temperature. The temperatures at which E'' and tanδ for nylon 11 show their maxima, at various frequencies, give rise to the dispersion map shown in Fig. 18. The straight line for E'' in this figure gives an activation energy of 68 kcal/mole, and the line for tanδ gives 65 kcal/mole.

Stress Relaxation and Birefringence Relaxation under Constant Strains

Before full-scale relaxation measurements were made, it was found that quenched films of nylon 11 and 12 show linear stress-strain and birefringence-strain relationships

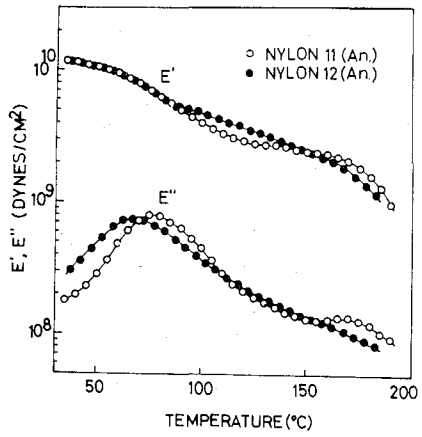

Fig. 14. Temperature dependence of the storage Young's modulus E' and loss modulus E'' at 110 Hz for the annealed films of nylon 11 and 12.

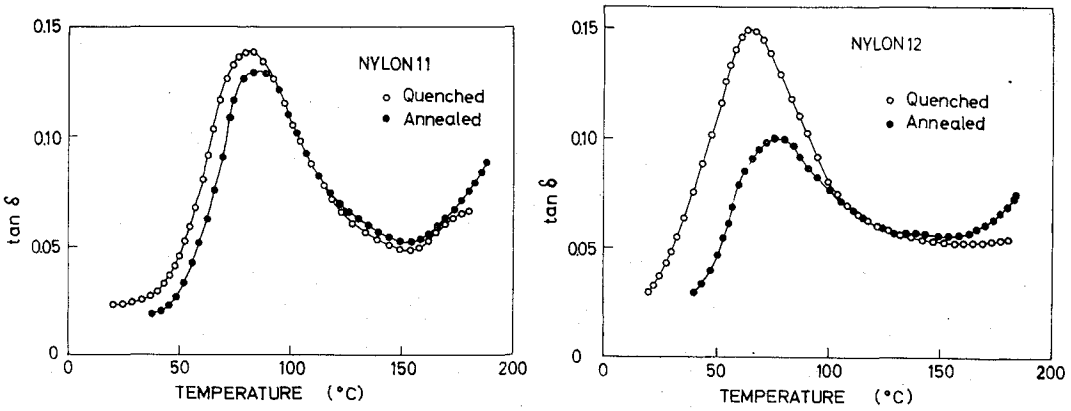

Fig. 15. Temperature dependence of tanδ at 110 Hz for the quenched and annealed films of nylon 11 and 12.

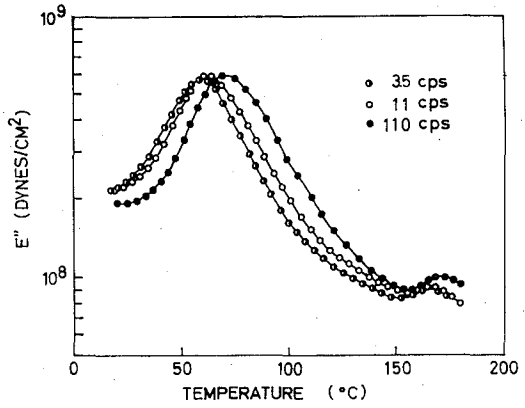

Fig. 16. Temperature dependence of E'' measured at 110 Hz, 11 Hz, and 3.5 Hz for the quenched nylon 11 film.

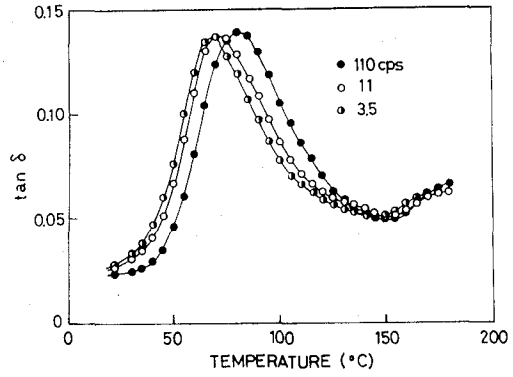

Fig. 17. Temperature dependence of tanδ measured at 110 Hz, 11 Hz, and 3.5 Hz for the quenched nylon 11 film.

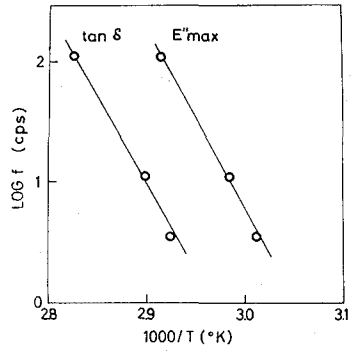

Fig. 18. The dispersion map for the quenched nylon 11 film.

only when the initial strains were lower than 2.5%. Therefore, all the relaxation experiments were carried out under constant strains less than this limiting value.

First, the quenched films of nylon 11 and 12 were elongated to about 2% at the highest speed of the tensile tester (400%/min) and then the stress relaxation and birefringence relaxation were measured at constant length, over a temperature range from 20° to 100°C. The time dependence of the strain-optical coefficient is shown in Figs. 19

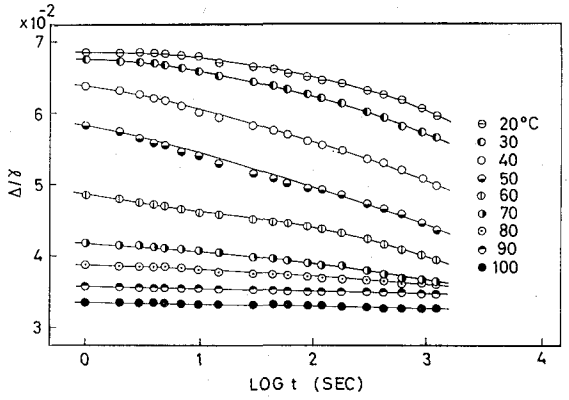

Fig. 19. The variation of strain-optical coefficient with time for the quenched nylon 11 film at various temperatures.

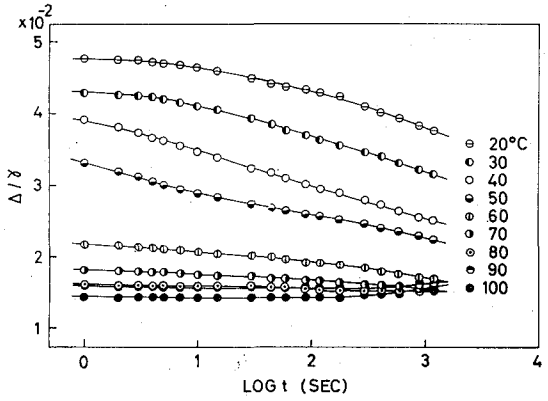

Fig. 20. The variation of strain-optical coefficient with time for the quenched nylon 12 film at various temperatures.

and 20 for the two nylons. It is evident from these figures that the strain-optical coefficient decreases with increasing time, but decreases especially rapidly at temperatures between 20° and 60°C. Above 70°C, the strain-optical coefficient becomes less dependent on time. An exception is nylon 12 at 90° and 100°C where the strain-optical coefficient increases with time at the long-time end. To understand this unusual behavior, several other properties were measured after the relaxation experiments at different temperatures, and it was found that the increases in the strain-optical coefficient for nylon 12 correlates with the increase in degree of crystallinity. Namely, the density of the sample specimens, as measured at 30°C following the relaxation measurements, is unchanged if the temperature is below 80°C, but it increases for temperatures in the range 90–100°C, as shown in Fig. 21. In the case of nylon 11, the density also increases at higher temperatures, but the strain-optical coefficient does not. This is probably due to the fact that the crystal transformation described above has the effect of decreasing the birefringence or strain-optical coefficient. This effect of the crystal transformation overrides the effect of the crystallinity and the net change is an increases of the strain-optical coefficient.

In order to make the temperature dependence of the strain-optical coefficient clearer, the coefficient at 1 sec was obtained from Figs. 19 and 20 and plotted against temperature

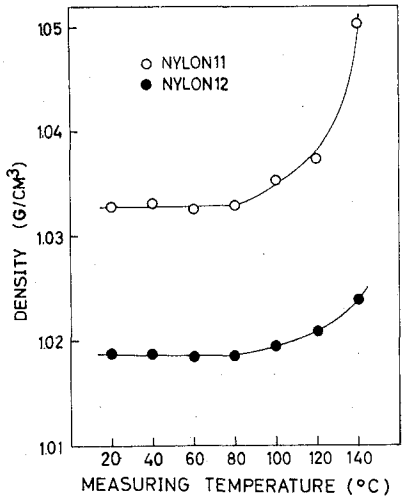

Fig. 21. The variation of density with measuring temperature.

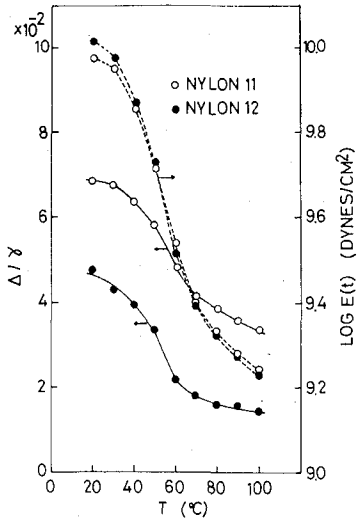

Fig. 22. Temperature dependence of the strain-optical coefficient and relaxation modulus at 1 sec. for the quenched films of nylon 11 and 12.

in Fig. 22. As may be seen in this figure, the strain-optical coefficient decreases continuously with temperature and the decrease is most prominent around 50°C.

Thus, the time and temperature dependences of the strain-optical coefficients for the nylons are quite different from those for polyethylene and polypropylene, which were studied previously. This suggests that there are some basic differences in the crystalline structure and in the orientation mechanisms between the nylons and the polyolefins.

It was found that time-temperature superposition could be applied to the time dependence curves for the strain-optical coefficient of the polyolefins[15~17]. Thus the superposition could be applied also to the curves at different temperatures, as is shown in Figs. 19 and 20. The curves below 50°C were satisfactorily superposed by horizontal shifts, while the curves at the higher temperatures were not; they could not be superposed even when we employed both horizontal and vertical shifts. Since the density of the films was

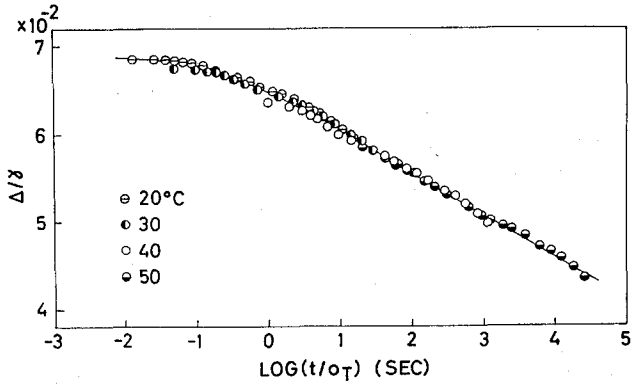

Fig. 23. Master curve of strain-optical coefficient for the quenched nylon 11 film at 40°C.

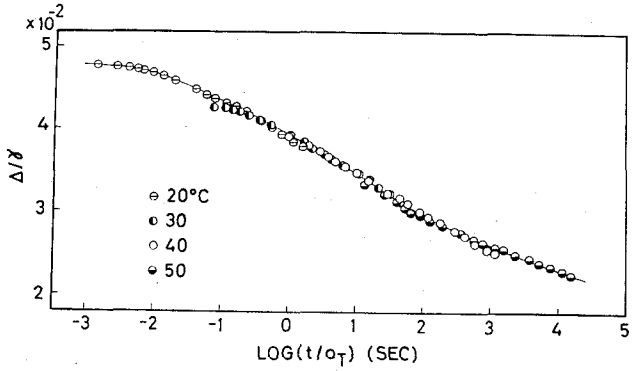

Fig. 24. Master curve of strain-optical coefficient for the quenched nylon 12 film at 40°C.

unchanged below 90°C, this failure of the superposition method is probably due to a change in humidity or of water content of the specimens. In general, the viscoelastic properties of nylons are affected strongly by humidity, as was emphasized in a previous paper,[18] and this seems to be true also for the rheo-optical properties. The master curves for the superposed strain-optical coefficients are shown in Figs. 23 and 24.

The shift factor o_T determined in the course of the superposition is plotted logarithmically against the reciprocal of absolute temperature $1/T$ in Fig. 25. The plots for nylon 11 and for nylon 12 give the same straight line, the slope of which gives an activation energy of 59.5 kcal/mole. This value of the activation energy is very close to the values of 65 and 68 kcal/mole which were obtained from the nylon 11 dispersion map for E'' and tanδ. But this value is about three times larger than that for polyethylene in the α_c-dispersion region. The good agreement of activation energies obtained from the viscoelastic and rheo-optical data indicates that the rheo-optical dispersion observed near 40–50°C is undoubtedly α-dispersion.

The corresponding stress relaxation curves, measured at different temperatures between 20° and 100°C for the quenched films, are shown in Figs. 26 and 27. The ordinate of these figures is the relaxation modulus $E(t)$. It is evident from these figures that $E(t)$ decreases with increasing time, as does the strain-optical coefficient. $E(t)$ also decreases

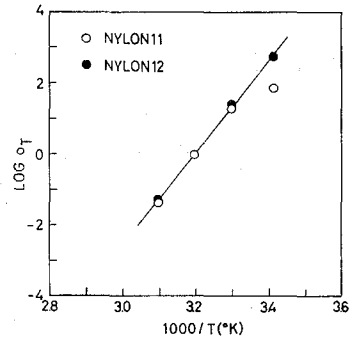

Fig. 25. Rheo-optical shift factor log a_T plotted against $1/T$ for the quenched films of nylon 11 and 12.

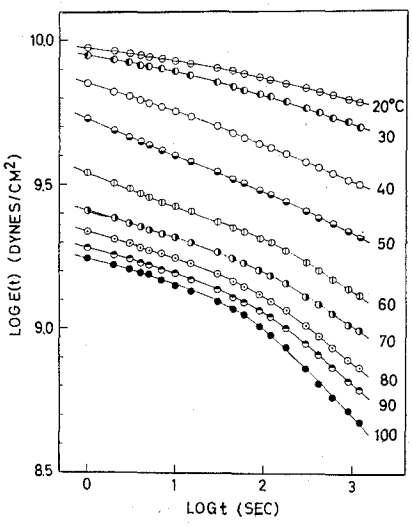

Fig. 26. The variation of relaxation modulus with time for the quenched nylon 11 film at various temperatures.

with increasing temperature in a manner similar to the strain-optical coefficient.

The time dependence curves of $E(t)$ below 40°C could be well superposed by a horizontal shift alone, while those above 60°C required both a horizontal and a vertical shift. The curves at 50° and 60°C could not be superposed at all. The master curves for $E(t)$ at reference temperatures of 40° and 80°C are given in Figs. 28 and 29. The master curve at 40°C is different in shape from that at 80°C, suggesting that the relaxation processes are not the same at the two temperatures. This effect is clearer when we look at the plot of shift factor a_T against $1/T$, as shown in Fig. 30. The straight line for temperatures lower than 50°C gives an activation energy of 63 kcal/mole, while that for the higher temperatures is 15 kcal/mole. The former agrees well with the value obtained from the rheo-optical and viscoelastic data mentioned above, indicating that this activation energy is for relaxation processes in the α-dispersion region. On the other hand, the lower activation energy at higher temperatures seems to correspond to some other relaxation processes; the nature of these is not clear yet. Figure 31 gives the vertical shift factor b_T plotted against temperature. b_T is much smaller than a_T and decreases rapidly at the lower temperatures

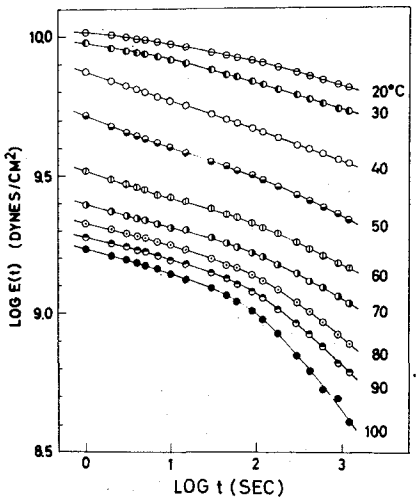

Fig. 27. The variation of relaxation modulus with time for the quenched nylon 12 film at various temperatures.

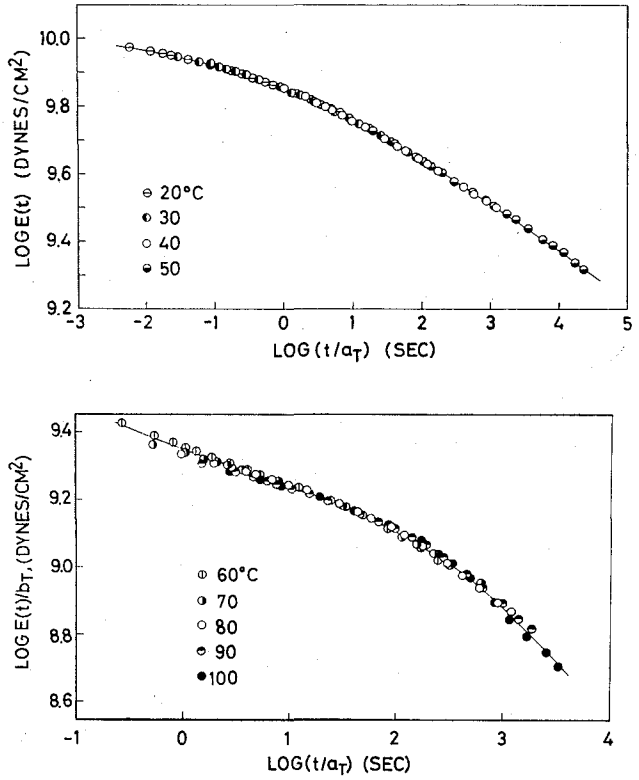

Fig. 28. Master curve of relaxation modulus for the quenched nylon 11 film at 40° and 80°C.

but slowly at the higher temperatures.

In our previous papers[7,19], we emphasized that the vertical shift for polyethylene was due to the variation of crystalline orientation with temperature rather than to the

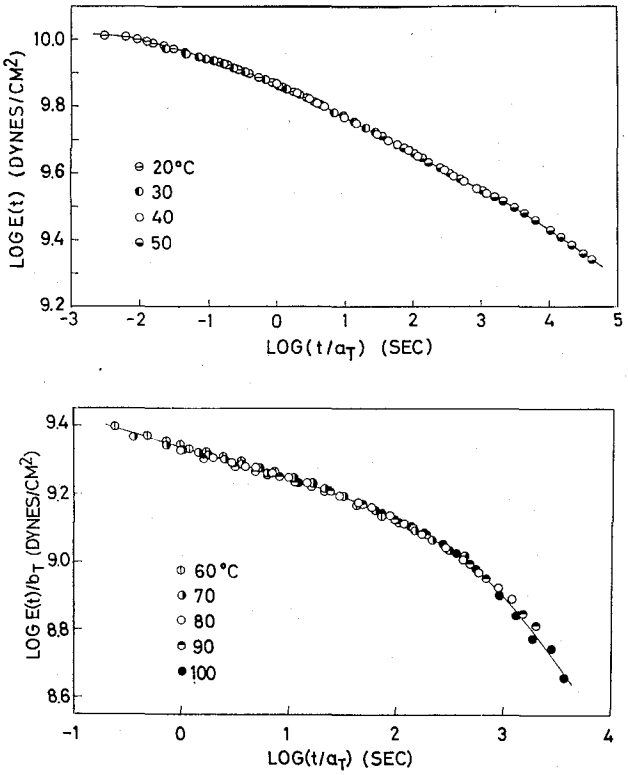

Fig. 29. Master curve of relaxation modulus for the quenched nylon 12 film at 40° and 80°C.

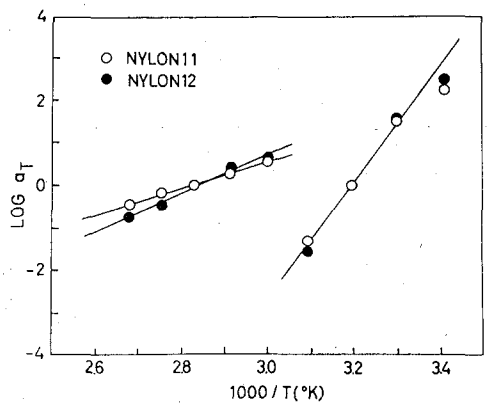

Fig. 30. Viscoelastic shift factor log a_T plotted against $1/T$ for the quenched films of nylon 11 and 12.

variation of degree of crystallinity as such. As mentioned above, the density and the degree of crystallinity of the nylons were almost constant over the temperature range covered by this study. Therefore, the vertical shift for the nylons also does not depend at all on the change in crystallinity.

The mechanical and rheo-optical relaxation spectra $H(\tau)$ and $(A_o'-B_o')$ for the

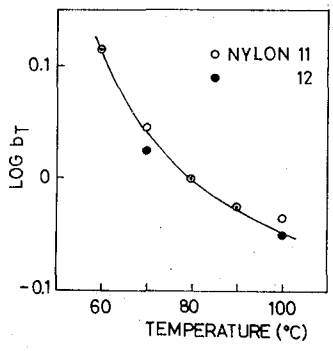

Fig. 31. Temperature dependence of the viscoelastic vertical shift factor log b_T for the quenched films of nylon 11 and 12.

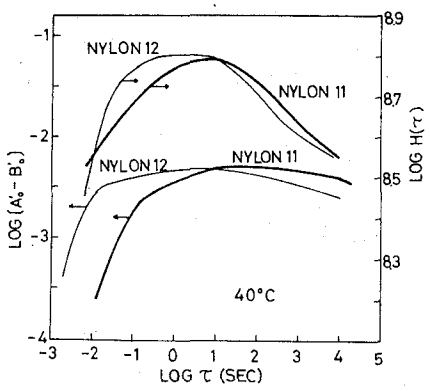

Fig. 32. Rheo-optical and viscoelastic relaxation spectra for the quenched films of nylon 11 and 12 at 40°C.

quenched films of nylon 11 and 12 were calculated from the master curves for $E(t)$ and Δ/γ. These results are plotted against relaxation time τ in Fig. 32. For polyethylene, B_0' was larger than A_0', but for the nylons B_0' is smaller. As is evident from this figure, the viscoelastic and rheo-optical relaxation spectra have peaks in the same region of time, indicating that the viscoelastic and rheo-optical α-dispersion can be attributed to the same relaxation mechanisms.

Infrared Dichroism

The infrared absorption bands which appear around 936 cm^{-1} for nylon 11 and around 950 cm^{-1} for nylon 12 seem to be crystalline bands similar to the 935 cm^{-1} band observed for nylon 6[20,21]. These bands have been discussed by Sandeman and Keller[20] as well as by other investigators. Sandeman and Keller mention in their paper that the 935 cm^{-1} band probably corresponds to a normal, in-phase vibration of the CONH group, and that the angle which the transition moment makes with the chain direction lies between 16° and 17°.

The absorbance of these bands, measured with films annealed for 30 min at various temperatures ranging from 100° to 190°C, is plotted against the density of the films in Fig. 33. It is evident from this figure that the absorbance A_c bears a linear relationship

to the density ρ and can thus be described by the following equations:

$$A_c=1.37\times10^3\ (\rho-1.019) \qquad \text{for nylon 11} \tag{1}$$

and

$$A_c=9.40\times10^2\ (\rho-0.988) \qquad \text{for nylon 12} \tag{2}$$

When $A_c=0$, these equations give the density ρ_a for the amorphous region; that is, at 30°C, $\rho_a=1.019$ g/cm^3 for nylon 11, and $\rho_a=0.998$ g/cm^3 for nylon 12. The former is somewhat larger than the value of 1.0098 obtained by Müller and Pflüger[22], and the latter is slightly larger than the value of 0.980 reported by the Toray group[23].

The quenched films of nylon 11 and 12 were elongated at a constant speed of 10%/min at 30°C, and the dichroic ratio D of the 936 cm^{-1} and 950 cm^{-1} bands was measured simultaneously with stress as a function of strain. The dichroic ratio-strain curves are given in Fig. 34. It is clear from this figure that D increases at first almost linearly with strain but levels off at larger strains.

The variation of D of the same bands with time under a constant strain (6.8% for

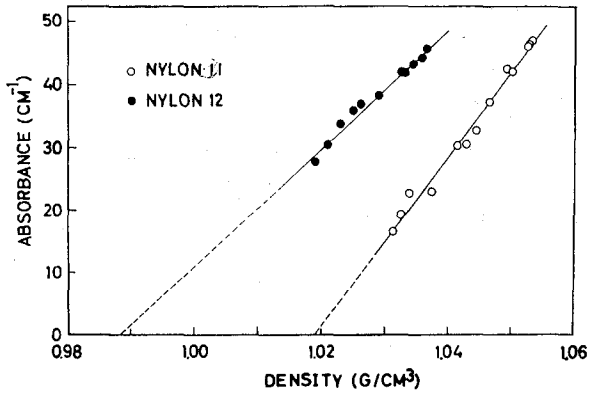

Fig. 33. The variation of absorbance of the 936 cm^{-1} (nylon 11) and 950 cm^{-1} (nylon 12) bands with density.

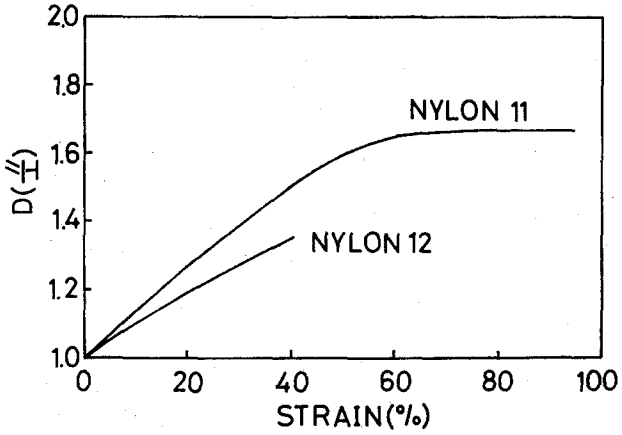

Fig. 34. The variation of dichroic ratio D for the 936 cm^{-1} and 950 cm^{-1} bands with strain.

nylon 11 and 5.3% for nylon 12) was measured at 40°C, around which the strain-optical coefficient decreases very rapidly. The results are shown in Fig. 35 as the solid lines. The broken lines in this figure represent the calculated values, as will be discussed later.

$(D-1)/(D+2)$ decreases with increasing time, indicating that the crystalline orientation relaxes with time. The strain-optical coefficient of the nylons also decreased with time as mentioned above. Therefore, the decrease in strain-optical coefficient is probably due to the decrease in orientation of the crystal c-axis relative to the stretching direction. This means that the crystalline orientation makes an important contribution to the total birefringence of the quenched films of nylon 11 and 12, though the degree of crystallinity of these materials is quite low. The decrease of the crystalline orientation function with time must override the increase of the amorphous orientation function. In order to make this point certain, the contribution from the amorphous orientation to the total birefringence should be determined.

For this purpose, the dichroic ratio D was measured for quenched films dyed with congo red. The orientation function F_D for the dye molecules and F_a for the polymer molecules in the amorphous region are given by[24]

$$F_D=\frac{D-1}{D+2}=\frac{1}{c}F_a, \tag{2}$$

where

$$c=\frac{3af_0}{(a_1-a_2)}. \tag{3}$$

a_1 and a_2 are the absorbancies of the dye molecules for light polarized parallel to, and perpendicular to, the absorbing axis, respectively; a is the average absorbance; and f_0 is

$$f_0=\frac{1}{2}(3\cos^2\alpha-1) \tag{4}$$

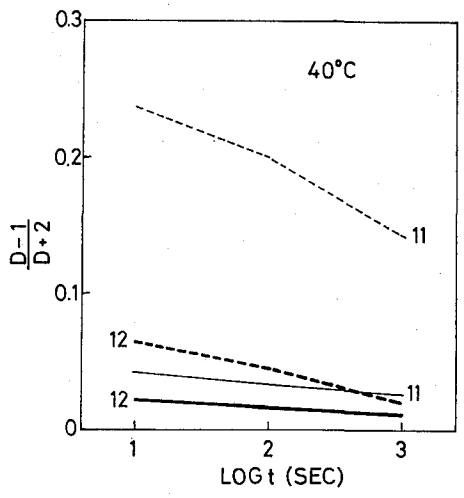

Fig. 35. The variation of $(D-1)/(D+2)$ with time for the quenched films of nylon 11 and 12. The solid lines represent experimental values, and the broken lines calculated ones.

where α is the angle that the principal axis makes with the orientation direction corresponding to complete orientation.

When f_0 is unchanged by elongation of the sample film, c is a constant independent of the elongation. When $a_2=0$ and $f_0=1$, c becomes unity. Usually c is larger than unity. In earlier work by Yamada and Stein,[3] c was assumed to be 1.5 for nylon 6.

The quenched films of nylon 11 and 12 were elongated at a constant speed of 10%/min at 40° and 80°C, and the variation of dichroic ratio was measured. The results are shown in Figs. 36 and 37. The ordinate of these figures is $F_D=(D-1)/(D+2)$. From these figures, it is clear that F_D initially increases with strain but levels off at larger strains. The trends shown by F_D are similar to those seen in the birefringence-strain curves shown above. F_D shows a higher value at 80°C than at 40°C, in marked contrast to the decrease in birefringence with increasing temperature. This means that the orientation function for the crystal c-axis, F_c, should decrease with increasing temperature.

The dichroic ratios after annealing for 30 min at high temperatures (nylon 11 at 180°C, nylon 12 at 175°C) were measured. The film specimens were elongated at 40°C at a constant speed of 10%/min. The results are given in Fig. 38. F_D increases with elongation and shows almost the same values for the two materials. Moreover, F_D for the annealed film of nylon 11 is almost equal to that for the quenched film, while F_D for the annealed film

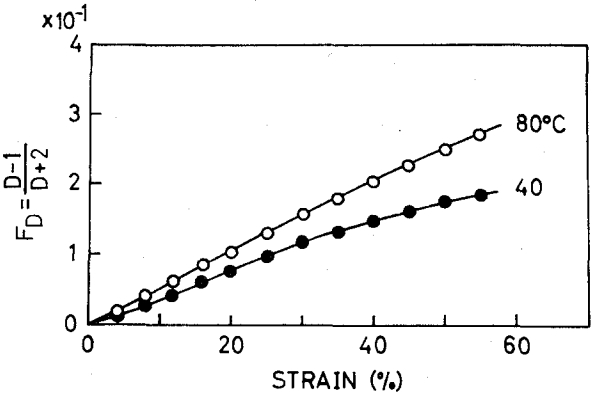

Fig. 36. The variation of F_D with strain for the quenched nylon 11 film at 40° and 80°C.

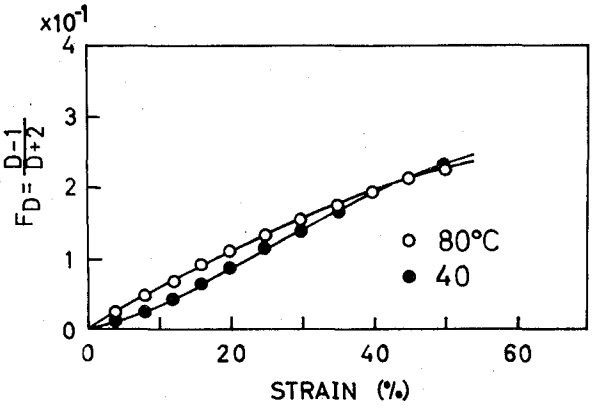

Fig. 37. The variation of F_D with strain for the quenched nylon 12 film at 40° and 80°C.

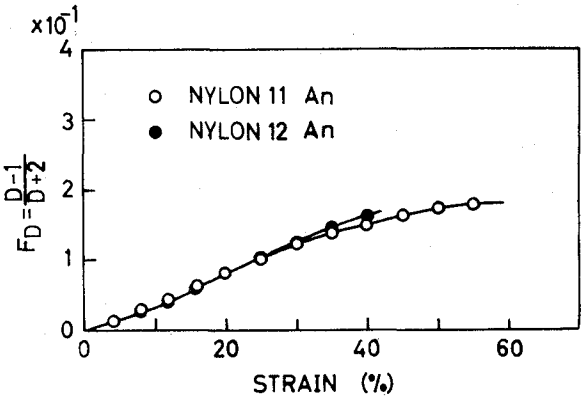

Fig. 38. The variation of F_D with strain for quenched films of nylon 11 and 12 at 40°C.

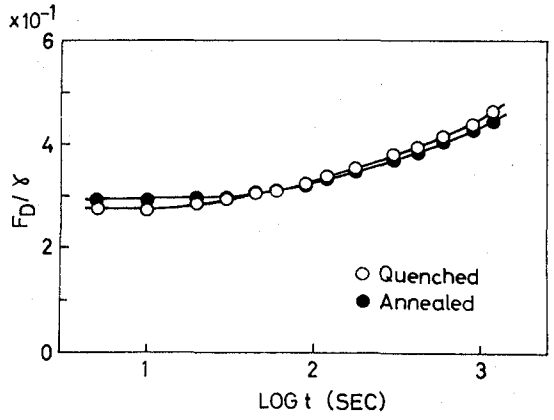

Fig. 39. The variation of F_D/γ with time for the quenched and annealed films of nylon 11 at 40°C.

of nylon 12 is lower than that for the quenched film. Such differences in F_D between nylon 11 and 12 are very similar to the differences observed in the birefringence measurements.

Novak and Vettegren[25] determined the crystalline and amorphous orientation functions of nylon 6 by employing the infrared dichroism method. From the variation of the orientation functions with strain, samples of lower crystallinities gave larger crystalline orientation functions, while the amorphous orientation function was independent of the crystallinity. In the above experimental results for nylon 11 and 12, F_D for low crystallinity was somewhat larger than that for high crystallinity. Summarizing these two results for nylon 6 and 12, it can be concluded that the decrease in birefringence caused by the annealing or by the increase in crystallinity is attributed mainly to the decrease in crystalline orientation functions.

For the quenched and annealed films of nylon 11 and 12, the relaxation of the dichroic ratio, under a constant elongation of 5%, was measured at 40°C. F_D/γ (where γ is the strain) is plotted against the logarithm of time in Figs. 39 and 40. As is evident from these figures, F_D/γ is almost constant at first but increases with increasing time. The increase in F_D with time was also observed for nylon 6 by Yamada and Stein[3]. Such an increase

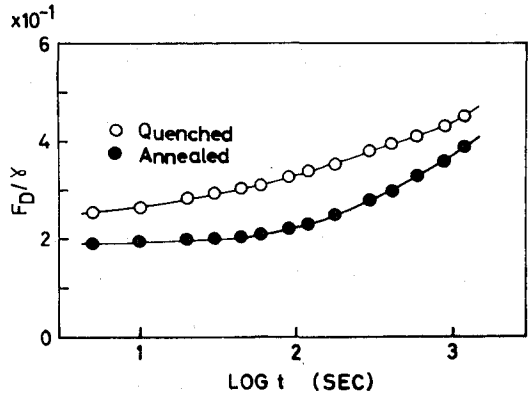

Fig. 40. The variation of F_D/γ with time for the quenched and annealed films of nylon 12 at 40°C.

in the dichroic ratio with time is just the reverse of the effects seen in the case of the strain-optical coefficient and the infrared dichroic ratios for the 936 and 950 cm^{-1} bands, where the measured quantities decrease with time.

Contributions of Amorphous and Crystalline Orientation to the Total Birefringence

As mentioned above, during the stress relaxation process, the birefringence and the orientation function of the crystal c-axis F_c=const·$(D-1)/(D+2)$ decreases with increasing time. On the other hand, the amorphous orientation function F_a (=const·F_D) increases with time. Neglecting the form birefringence, we can consider that the total birefringence is the sum of contributions from the crystalline and amorphous regions. Thus the fact that the total birefringence decreases with time means that the increase in amorphous orientation cannot compensate for the decrease in crystalline orientation. As mentioned above, the time-scales employed in this study cover the region of the primary or α-dispersion. It is usually believed that the α-dispersion originates from co-operative motions of molecular segments or submolecules. However, for crystalline polymers, such as the polyolefins studied before, the crystalline orientation makes an important contribution to the rheo-optical properties; the crystalline orientation is in fact a determining factor in the sense that the time dependence of the rheo-optical properties, such as birefringence, is determined by the crystalline orientation and the amorphous orientation cannot override this response.

Comparing the time and temperature dependences of the rheo-optical properties of the nylons with those for the polyolefins, we notice that these two materials show similar responses in the sense that the crystalline orientation plays an important role. This can be said, for at least, the α-dispersion region in nylon and for the α_c-dispersion region in polyolefins. There is, however, a striking difference in the mechanisms of crystalline orientation between the two materials. As mentioned in the introduction, the rheo-optical behavior of the polyolefins can be well explained by three mechanisms. But in the case of the nylons, one of the mechanisms, orientation of crystals in the spherulites, is missing. This mechanism causes the increase in birefringence and the increase of the orientation function of the c-axis with time during the stress relaxation measurements. The molecular

interpretation of this mechanism is not satisfactory at the present stage. Some investigators consider that the crystalline orientation occurs by slippage of crystal blocks past each other in the lamellae[26,27]. If such an irreversible change occurs, a film specimen used once for the relaxation measurement should change its spherulitic structure, and hence should manifest different birefringence behavior in repeated measurements. However, if one carries out relaxation experiments only at small strains, this irreversible effect is not observed.

When a spherulite in polyethylene, as an example, deforms as a unit upon sudden stretching, most lamellae in it are subjected mainly to stretching in the direction of its length as well as bending in the direction of the stretching. By such a process, the crystal c-axis orients perpendicular to the stretching direction. As time elapses, this orientation relaxes, and the c-axis reorients to the direction of the stretching, increasing the orientation function F_c, or the birefringence Δ, with time. But the increase in F_c or Δ observed experimentally is larger than that expected from such a reorientation of the c-axis. Therefore, some other reversible process must be occurring simultaneously such that the c-axis is oriented to the stretching direction even more. The only process of this type that the authors can imagine is the local twisting or untwisting of the lamellae, by which the c-axis is oriented to the stretching direction preferentially. Such a process can probably take place very easily in spherulites of polyolefins but not in those of nylons, because the lamellae in nylons have steady structure probably due to a high cohesive energy or strong hydrogen bonding between the molecules in the crystallites.

Returning to the major theme of the analysis we assume that the total birefringence Δ is the sum of contribution from the crystalline and amorphous regions as follows:[24,19]

$$\Delta=\Delta_c+\Delta_a=X_c\Delta_c^\circ F_c+(1-X_c)\Delta_a^\circ F_a$$

where X_c is the degree of crystallinity, F_a is the amorphous orientation function, and Δ_c° and Δ_a° are, respectively, the intrinsic birefringences for perfectly oriented crystals and amorphous molecular chains. According to Fig. 22, Δ/γ for the quenched film of nylon 11 decreases from 6.1×10^{-2} at 10 sec to 5.1×10^{-2} at 1000 sec. Correspondingly, Δ_a increases from 0.020 to 0.032 in the same range of time, if we assume

$$X_c=0.23,$$

$$\Delta_c^\circ=\Delta_a^\circ=0.060,$$

and

$$F_a=1.0F_D.$$

Subtracting this contribution of the amorphous orientation Δ_a from the total birefringence, we can obtain Δ_c, and hence F_c. F_c thus evaluated for nylon 11 was assumed further to be equal to $(D-1)/(D+2)$ and plotted against time in Fig. 35 (the thinner broken line). Similar evaluation of $(D-1)/(D+2)$ was carried out also for nylon 12, and the result is also shown in the same figure (the thicker broken line). As is evident from this figure, the calculated values of $(D-1)/(D+2)$ are much higher than the experimental values (the solid lines) and decrease more rapidly with time. Possible reasons for this discrepancy between the calculated and experimental values are as follows:

(a) Accurate determinations of D under small strains are difficult.

(b) Form birefringence cannot be ignored.

(c) The simple two-phase model for the total birefringence is not valid for nylon. Even if experimental errors in the measurements of D are large, they cannot explain the large discrepancy mentioned above. Moreover, the variation of D with strain during the constant rate of strain experiments shown in Fig. 34 is also rather small, even though the strain becomes quite large. Therefore, reason (a) should probably be rejected. Also the possibility that the assumptions about the intrinsic birefringences, F_c and F_a are at fault can be rejected. Published data which can affirm or deny reason (b) and (c) do not seem to be available. These will be an important problems for further investigation.

ACKNOWLEDGMENT

This study was supported, in part, by a grant for scientific research (Kagaku Kenkyuhi Hojokin) from the Ministry of Education. We are indebted to Dr. Akira Kishimoto (Toyo Seikan Co., Ltd.) for the nylon films.

REFERENCES

(1) For instance, Onogi Laboratory, "*Rheo-Optical Properties of High Polymers*, 1961–1970" (1970); A. Tanaka, E. P. Chang, B. Delf, I. Kimura, and R. S. Stein, *J. Polym. Sci., Polym. Phys. Ed.*, **11**, 1891 (1973).
(2) R. Yamada, C. Hayashi, and S. Onogi, *Zairyo*, **13**, 117 (1964).
(3) R. Yamada and R. S. Stein, *J. Polym. Sci.*, **B2**, 1131 (1964).
(4) R. Yamada, C. Hayashi, and S. Onogi, Preprints of Scientific Papers, International Symposium on Macromolecular Chem., Tokyo-Kyoto, **8**, 161 (1966).
(5) S. Onogi and T. Asada, "*Progress in Polymer Science, Japan*", Vol. 2, M. Imoto and S. Onogi ed., Kodansha, Tokyo (1971) pp. 261–328.
(6) S. Onogi, H. Kawai, and T. Asada, *Kobunshi Kagaku*, **21**, 746 (1964).
(7) S. Onogi, T. Sato, T. Asada, and Y. Fukui, *J. Polym. Sci., A-2*, **8**, 1211 (1970).
(8) W. P. Slichter, *J. Polym. Sci.*, **36**, 259 (1959).
(9) K. Little, Brit. *J. Appl. Phys.*, **10**, 225 (1959).
(10) W. Ruland, *Polymer*, **5**, 89 (1964).
(11) Y. Kinoshita, *Makromol. Chem.*, **33**, 1 (1959).
(12) K. Monobe, K. Shimamura, M. Tabuchi, and Y. Fujisawa, Paper presented at the 13th Symposium of the Society of Polymer Sci., Japan, Nov. 12–14, Tokyo (1964).
(13) T. Sasaki, M. Ogawa, and T. Suzuki, Paper presented at the 14th Symposium of the Society of Polymer Sci., Japan, Oct. 5–7, Kyoto (1965).
(14) H. Arimoto, *Kobunshi Kagaku*, **19**, (1962).
(15) Y. Fukui, T. Sato, M. Ushirokawa, T. Asada, and S. Onogi, *J. Polym. Sci., A-2*, **8**, 1195 (1970).
(16) S. Onogi, T. Asada, Y. Fukui, and T. Fujisawa, *J. Polym. Sci., A-2*, **5**, 1067 (1967).
(17) S. Onogi, Y. Fukui, T. Asada, and Y. Naganuma, *Proc. 5th Intern. Congr. Rheology*, **4**, 87 (1970).
(18) S. Onogi, K. Sasaguri, T. Adachi, and S. Ogihara, *J. Polym. Sci.*, **58**, 1 (1962).
(19) Y. Fukui, T. Asada, and S. Onogi, *Polymer J.*, **3**, 100 (1972).
(20) I. Sandeman, and A. Keller, *J. Polym. Sci.*, **19**, 401 (1956).
(21) H. Arimoto, *Kobunshi Kagaku*, **19**, 205 (1962).
(22) A. Müller, and R. Pflüger, *Kunststoffe*, **50**, 203 (1960).
(23) Private communication from Toray Co.
(24) R. S. Stein, "*Rheology, Theory and Application*, Vol. V", F. R. Eirich ed., Academic Press, New York (1969) Chap. 6.
(25) I. I. Novak, and V. I. Vettegren, *Vysokomol. soyed.*, **6**, 706 (1964).
(26) T. Oda, N. Sakaguchi, and H. Kawai, *J. Polym. Sci.*, **C15**, 223 (1966).
(27) M. Takayanagi, and T. Matsuo, *J. Macromol. Sci., B-1*, **3**, 407 (1967).